Research Article BEU Fen Bilimleri Dergisi 15(2): 884-897 (2026) DOI: 10.17798/bitlisfen.1842996

BİTLİS EREN UNIVERSITY
FEN BİLİMLERİ DERGİSİ
ISSN: 2147-3129 / e-ISSN: 2147-3188

ENHANCED TRANSIENT PERFORMANCE OF MICRO-ROBOTIC SYSTEMS VIA SFOA-BASED PID TUNING

Muhammet İsmail GÜNGÖR [1], **Davut İZCİ** [1*], Serdar EKİNCİ [2], Ehab GHITH [3]

[1] *Department of Electrical and Electronic Engineering, Bursa Uludag University, Bursa, Turkey*
[2] *Department of Computer Engineering, Bitlis Eren University, Bitlis, Turkey*
[3] *Faculty of Engineering, Ain Shams University, Cairo, Egypt*
**** Corresponding Author:*** *davutizci@uludag.edu.tr*

Article Info

Received: *December 16, 2025*
Revised: *April 30, 2026*
Accepted: *April 30, 2026*

Keywords
Micro-robotic Position Control, Starfish Optimization Algorithm, PID Controller Tuning, Magnetic Actuation, Transient Performance, Optimization.

ABSTRACT

Precise position control of magnetically actuated micro-robotic systems is challenging due to viscous damping, parameter sensitivity, and the requirement for high transient accuracy without overshoot. This study presents an optimization-based control framework for enhancing transient and steady-state performance of a magnetically actuated micro-robotic position control system. The system dynamics are modeled based on magnetic force and viscous drag interactions on paramagnetic micro-particles suspended in fluid, yielding a second-order representation suitable for controller design. A proportional–integral–derivative (PID) controller regulates particle position, with parameters optimally tuned using the starfish optimization algorithm (SFOA), a bio-inspired metaheuristic that balances global exploration and local exploitation through biologically motivated movement, preying, and regeneration mechanisms. The tuning process is guided by the integral of squared time multiplied by squared error performance index, which suppresses late-stage tracking errors and promotes smooth transient behavior. Simulation studies are conducted for a 1000 µm step reference input, with the optimization independently repeated 25 times to assess robustness and consistency. Results demonstrate strong convergence reliability, with tightly clustered objective function values and low standard deviation across runs. Time-domain analyses confirm that the SFOA-tuned PID controller achieves a smooth, monotonic, overshoot-free response with the shortest rise and settling times compared to PID controllers tuned by arithmetic optimization, jellyfish search optimization, Harris hawks optimization, and a hybrid arithmetic–rat swarm approach. These findings establish the proposed method as an effective and reliable solution for high-precision micro-robotic positioning where overshoot-free operation and consistent transient performance are critically important.

1. INTRODUCTION

Micro-robotic systems have attracted significant attention in recent years due to their potential applications in biomedical engineering, micro-manipulation, targeted drug delivery, and lab-on-a-chip technologies [1–3]. In such applications, precise and reliable position control is a fundamental requirement, as even minor tracking errors can degrade performance or cause task failure. Magnetically actuated micro-robotic platforms that rely on externally generated magnetic fields to manipulate paramagnetic micro-particles suspended in fluid media offer several advantages, including wireless actuation, biocompatibility, and suitability for operation in enclosed or sensitive environments [4–6]. However, controlling these systems remains challenging due to strong viscous damping, high sensitivity to parameter variations, and nonlinear interactions between magnetic forces and fluid dynamics.

The dynamic behavior of magnetically actuated micro-particles is primarily governed by the balance between magnetic forces and viscous drag under low Reynolds number conditions. As a result, the system exhibits slow transient responses and is highly susceptible to oscillations or overshoot if the control strategy is not carefully designed. Classical control approaches, particularly proportional–

 License: CC BY-NC 4.0

integral–derivative (PID) controllers, continue to be widely adopted in micro-positioning applications due to their structural simplicity, robustness, and ease of implementation [7–9]. Nevertheless, the performance of PID-controlled micro-robotic systems is strongly dependent on the appropriate selection of controller gains [10]. Conventional tuning techniques often fail to provide satisfactory performance across varying operating conditions and may lead to excessive overshoot, prolonged settling times, or poor robustness [11].

In recent years, metaheuristic optimization algorithms have been increasingly employed to address controller tuning problems in complex and nonlinear systems [12–14]. These algorithms offer the ability to explore large search spaces without relying on gradient information and have demonstrated promising results in control-oriented optimization tasks. Despite these advantages, the effectiveness of a metaheuristic-based tuning approach is closely related to its ability to balance global exploration and local exploitation while maintaining convergence stability [15]. Moreover, for micro-robotic positioning applications, it is essential that the optimization process explicitly accounts for time-domain performance requirements, particularly overshoot suppression and smooth convergence to the desired position [16].

Motivated by these considerations, this study proposes an optimization-based PID tuning framework for magnetically actuated micro-robotic position control systems using the starfish optimization algorithm (SFOA) [17]. The SFOA is a bio-inspired metaheuristic that models the arm-based movement, preying behavior, and regenerative capability of starfish to achieve an effective balance between exploration and exploitation [18]. In the proposed framework, the SFOA is integrated as an external optimization layer within the closed-loop control structure, allowing the PID parameters to be tuned directly based on the system's dynamic response. To guide the optimization process toward overshoot-free and well-damped behavior, the integral of squared time multiplied by error squared performance index [19] is adopted as the objective function. This criterion penalizes late-stage tracking errors more severely and promotes smooth transient responses.

The effectiveness of the proposed approach is evaluated through comprehensive simulation studies conducted on a magnetically actuated micro-robotic position control system modeled using fundamental physical principles. All analyses are performed for a step reference change of 1000 μm, representing a realistic and practically relevant positioning task. The optimization procedure is independently repeated multiple times to assess robustness and convergence reliability, and the obtained results are statistically analyzed. Furthermore, the performance of the proposed method is comparatively evaluated against PID controllers tuned using several well-established metaheuristic algorithms, including arithmetic optimization [19], jellyfish search optimization [19], Harris hawks optimization [19], and a hybrid arithmetic–rat swarm optimization approach [19]. In contrast to recent hybrid metaheuristic-based PID tuning approaches for micro-robotic position control, such as the hybrid framework reported in [19], the present study employs a single structured SFOA without algorithmic hybridization. This design choice significantly reduces computational overhead while preserving strong exploration–exploitation balance. The results demonstrate that the proposed single-algorithm framework achieves both lower objective function values and overshoot-free transient behavior with tighter statistical consistency, indicating that hybridization is not strictly necessary to obtain superior control-oriented optimization performance for this class of systems.

The remainder of this paper is organized as follows. Section 2 presents the modeling of the micro-robotic position control system based on magnetic actuation and viscous drag dynamics. Section 3 describes the Starfish Optimization Algorithm and its underlying mechanisms in detail. Section 4 introduces the adopted control structure, including the PID controller formulation, objective function definition, and implementation framework. Section 5 reports and discusses the simulation results, including statistical analyses, objective function evolution, and time-domain performance comparisons. Finally, Section 6 concludes the paper and outlines potential directions for future research.

2. MICRO-ROBOTIC POSITION CONTROL SYSTEM

The micro-robotic position control system under consideration is based on the manipulation of paramagnetic micro-particles suspended in a viscous liquid medium [20]. The particles are fabricated

from iron oxide and dispersed in lactic acid, with each particle having an approximate diameter of $100\ \mu m$. The motion of these micro-particles is governed by the interaction between magnetic forces generated by external electromagnetic coils and viscous drag forces arising from the surrounding fluid. The velocity of the micro-particles is influenced by two dominant physical effects: the magnetic force induced by the spatial variation of the magnetic field and the viscous drag force opposing the motion. When these forces reach equilibrium, the particle acceleration becomes zero, and the micro-particle attains its maximum steady-state velocity. The magnetic force acting on a paramagnetic particle is defined as [19]:

$$F = \nabla \alpha_p V_p B^2 \tag{1}$$

where V_p denotes the particle volume, B represents the magnetic flux density, and α_p is the magnetic susceptibility of the particle. The magnetic field gradient depends on both spatial position and time, whereas $\alpha_p$and $V_p$are treated as constant parameters.

Assuming perfectly spherical micro-particles, the particle volume can be expressed in terms of the particle radius r_p. Substituting this geometric relationship into the magnetic force expression yields the following.

$$F = \frac{4}{3}\pi \alpha_p r_p^3 \nabla B^2 \tag{2}$$

The opposing viscous force acting on the particle is modeled using Stokes' drag law, which is appropriate under low Reynolds number conditions. The drag force is given by:

$$F_d = -6\pi\eta r_p v \tag{3}$$

where η denotes the dynamic viscosity of the fluid and $v$represents the linear velocity of the micro-particle.

The dynamic behavior of the particle is governed by Newton's second law of motion, which relates the net force acting on the particle to its mass m_p and acceleration a_p.

$$\sum F = m_p a_p \tag{4}$$

By combining the magnetic force and viscous drag force expressions, the governing force balance equation is obtained as follows.

$$\frac{4}{3}\pi \alpha_p r_p^3 \nabla B^2 - 6\pi\eta r_p v = m_p a_p \tag{5}$$

Rearranging this expression with respect to the particle velocity yields the following.

$$v = \frac{\frac{4}{3}\pi \alpha_p r_p^3 \nabla B^2 - m_p a_p}{6\pi\eta r_p} \tag{6}$$

The maximum particle velocity is achieved when the acceleration term approaches zero, corresponding to steady-state motion. Under this condition, the maximum attainable velocity of the micro-particle is expressed as follows.

$$v_m = \frac{2}{9}\frac{\alpha_p r_p^2}{\eta}\nabla B^2 \tag{7}$$

For control and modeling purposes, the micro-particle motion is represented using a continuous-time dynamic formulation. The applied magnetic force F_m acts as the system input, while the particle displacement x is treated as the output. Assuming laminar flow conditions and low Reynolds numbers, the viscous drag coefficient is denoted by C_d. All variables in the following equation represent time-dependent continuous-time signals. The resulting equation of motion is given by:

$$m\ddot{x} + C_d\dot{x} = F_m \tag{8}$$

where m represents the effective mass of the micro-particle, $\dot{x}$ denotes velocity, and $\ddot{x}$ denotes acceleration.

Taking the Laplace transform of the dynamic equation under zero initial conditions leads to the transfer function representation of the micro-robotic position control system as given below [19].

$$\frac{X(s)}{F_m(s)} = \frac{1}{ms^2 + C_d s} \tag{9}$$

This second-order model captures the essential dynamics of the micro-particle motion under magnetic actuation and viscous damping. It provides a suitable mathematical foundation for the subsequent design and optimization of advanced control strategies aimed at precise micro-robotic position regulation.

3. STARFISH OPTIMIZATION ALGORITHM

The starfish optimization algorithm (SFOA) is a bio-inspired population-based metaheuristic developed to address complex and nonlinear optimization problems [21]. The method is conceptually derived from the observed behavioral mechanisms of starfish, particularly their arm-based movement, hunting strategy, and regenerative capability. These mechanisms are mathematically modeled to establish a dynamic balance between global exploration and local exploitation throughout the optimization process.

3.1. Population Initialization

At the initial stage, a population consisting of N starfish is generated. Each starfish represents a candidate solution, whose position is defined in a D-dimensional search space. The initial positions are uniformly distributed within the predefined lower and upper bounds of each decision variable according to Eq. (10) [21]:

$$X_{ij} = l_j + r \cdot (u_j - l_j), r \in (0,1) \tag{10}$$

where l_j and u_j denote the lower and upper bounds of the j-th dimension, respectively, and r is a uniformly distributed random number.

3.2. Exploration Phase

The exploration mechanism of SFOA is designed to adapt according to the dimensionality of the optimization problem. This adaptive behavior enables efficient coverage of the search space while preventing premature convergence.

For high-dimensional problems ($D > 5$), a multidirectional search strategy is employed, inspired by the radial movement of starfish arms. The position update rule is expressed as [21]:

$$Y_{i,p}^{(t)} = \begin{cases} X_{i,p}^{(t)} + \alpha\left(X_{best,p}^{(t)} - X_{i,p}^{(t)}\right)cos\,(\theta), & r \le 0.5 \\ X_{i,p}^{(t)} - \alpha\left(X_{best,p}^{(t)} - X_{i,p}^{(t)}\right)sin\,(\theta), & r > 0.5 \end{cases} \tag{11}$$

where $\alpha = (2r-1)\pi$, $r \in (0,1)$, and $\theta = \frac{\pi}{2}\left(\frac{t}{t_{\max}}\right)$. This formulation allows candidate solutions to oscillate around the current best solution while maintaining sufficient diversity during early iterations.

For low-dimensional search spaces ($D \leq 5$), a simplified directional movement is adopted to enhance computational efficiency. The update equation is defined as [21]:

$$Y_{i,q}^{(t)} = E^t X_{i,p}^{(t)} + A_1\left(X_{k_1,p}^{(t)} - X_{i,p}^{(t)}\right) + A_2\left(X_{k_2,p}^{(t)} - X_{i,p}^{(t)}\right) \tag{12}$$

where k_1 and k_2 are randomly selected indices, and A_1 and A_2 are random coefficients. The time-varying energy term E^t is given by [21]:

$$E^t = \left(\frac{t_{max} - t}{t_{max}}\right) cos(\theta) \tag{13}$$

which gradually reduces exploratory behavior as the iteration count increases.

3.3. Exploitation Phase

As the algorithm progresses, exploitation becomes dominant in order to refine promising solutions. This phase incorporates both preying and regeneration behaviors observed in starfish.

Preying mechanism: During the preying step, each starfish adjusts its position using directional vectors oriented toward the current best solution [21]:

$$Y_i^{(t)} = X_i^{(t)} + r_1 d_{m1} + r_2 d_{m2} \tag{14}$$

where r_1 and r_2 are random scalars in $(0, 1)$, and d_{m1} and d_{m2} represent distance vectors between the current solution and the global best solution along different dimensions. This operation intensifies the local search around high-quality regions of the search space.

Regeneration mechanism: To further enhance convergence stability, a regeneration step is applied, particularly to the last starfish in the population. This mechanism models the biological regeneration capability of starfish and is formulated as follows [21].

$$Y_i^{(t)} = e^{\left(-\frac{t \times N}{t_{max}}\right)} X_i^{(t)} \tag{15}$$

This exponential decay factor progressively dampens the movement amplitude, enabling fine-grained solution refinement in later iterations.

Boundary handling: To ensure feasibility, any solution that violates the predefined search bounds is corrected using a saturation-based boundary control scheme [21]:

$$X_i^{(t+1)} = \begin{cases} Y_i^{(t)}, & l \leq Y_i^{(t)} \leq u \\ l, & Y_i^{(t)} < l \\ u, & Y_i^{(t)} > u \end{cases} \tag{16}$$

where l and u denote the lower and upper bounds of the decision variables.

3.4. Termination Criterion

The iterative process continues until a stopping condition is satisfied, which is typically defined by the maximum number of iterations $t_{\max}$. Upon termination, the best solution identified throughout the optimization process is reported as the final output. The pseudocode of the SFOA is given in Algorithm 1. After each candidate update, the objective function is re-evaluated. If the new position produces a lower cost value, it replaces the previous position of that starfish (greedy selection). At the end of each iteration, all candidate fitness values are compared and the global best solution X_{best} is updated if a better solution is found. This memory mechanism ensures monotonic improvement of the best-so-far solution and supports stable convergence toward the global optimum.

Algorithm 1. The pseudocode of SFOA

```
Input:
    f(·): objective function
    N: number of starfish
    D: problem dimension
    l, u: lower and upper bounds
    t_max: maximum number of iterations
Output:
    X_best: best solution
    f_best: best fitness value
Initialize population X using Eq. (8)
Evaluate the fitness of all starfish
Determine initial best solution X_best
for t = 1 to t_max do
      Compute θ and energy term E^t using Eqs. (9) and (11)
      for each starfish i = 1 to N do
        ▷ Exploration Phase
          if D > 5 then
              Update position using high-dimensional exploration (Eq. (9))
          else
              Update position using low-dimensional exploration (Eq. (10))
          end if
        ▷ Exploitation Phase
          Apply the preying mechanism using Eq. (12)
          if i is the last starfish then
              Apply the regeneration mechanism using Eq. (13)
          end if
        ▷ Boundary Handling
          Correct boundary violations using Eq. (14)
        ▷ Selection
          Evaluate new solution
          Update starfish position if fitness improves
      end for
      Update global best solution
end for
return X_best, f_best
```

4. ADOPTED CONTROL STRUCTURE

4.1. PID Controller

To regulate the position of the micro-robotic system, a classical PID controller is employed due to its simplicity, robustness, and well-established effectiveness in motion control applications [22]. The PID controller generates the control input by processing the error signal, which is defined as the difference between the reference position and the measured system output. As illustrated in Figure 1, the reference signal is compared with the feedback signal to produce the tracking error. This error is simultaneously processed through three parallel control paths corresponding to the proportional, integral, and derivative actions. The weighted outputs of these paths are then summed to form the control signal applied to the plant.

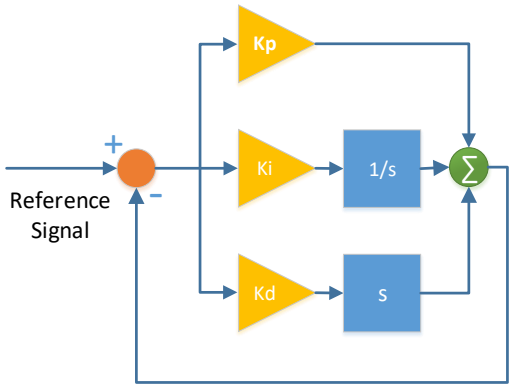


Figure 1. Schematic structure of PID controller

The control law of the PID controller in the time domain is expressed as:

$$u(t) = K_p e(t) + K_i \int_0^t e(\tau)\, d\tau + K_d \frac{de(t)}{dt} \tag{17}$$

where $e(t)$denotes the tracking error, $u(t)$represents the control input, and K_p, K_i, and $K_d$are the proportional, integral, and derivative gains, respectively.

In the block diagram, the proportional path directly amplifies the instantaneous error through the gain K_p, providing an immediate corrective response. The integral path consists of the gain $K_i$followed by an integrator block $1/s$, which accumulates the error over time and eliminates steady-state offset. The derivative path includes the gain $K_d$and a differentiator block s, which anticipates the system response by reacting to the rate of change of the error and enhances damping characteristics. For analysis and controller synthesis, the PID controller can be represented in the Laplace domain as follows [23].

$$C(s) = K_p + \frac{K_i}{s} + K_d s \tag{18}$$

This transfer function clearly reflects the three control actions depicted in the figure, where each term contributes to shaping the closed-loop dynamics. The summation block at the controller output combines the proportional, integral, and derivative components to generate a single control force signal. When integrated with the micro-robotic position control system model, the PID controller aims to achieve accurate reference tracking, reduced settling time, minimal overshoot, and robust disturbance rejection. The controller gains are typically tuned to balance transient performance and steady-state accuracy, making the PID structure particularly suitable for precise micro-scale position regulation.

4.2. Objective Function Formulation

In order to quantitatively evaluate the closed-loop performance of the micro-robotic position control system, a time-domain error–based performance index is adopted. In this study, the integral of squared time multiplied by error squared (ISTES) [19] criterion is selected as the objective function due to its proven effectiveness in achieving high tracking accuracy and enhanced transient performance, as widely reported in the control literature. The ISTES objective function penalizes tracking errors more severely as time progresses by incorporating a quadratic time-weighting term. As a result, early transient deviations are tolerated to a limited extent, while persistent or late-occurring errors are strongly suppressed. This characteristic encourages rapid convergence, reduced settling time, and improved stability of the closed-loop system. The mathematical definition of the ISTES performance index is given by [19]:

$$ISTES = \int_0^\infty t^2\, e^2(t)\, dt \tag{19}$$

where $e(t)$ represents the instantaneous tracking error between the reference signal and the system output. By minimizing this criterion, the controller is driven to reduce both the magnitude and duration of the error, leading to a fast and well-damped system response.

4.3. Implementation Framework

The implementation framework of the proposed control strategy is illustrated in Figure 2. The structure integrates the SFOA with a PID-controlled micro-robotic position control system in a closed-loop configuration. As shown in Figure 2, the reference signal is compared with the measured output of the plant to generate the error signal. This error serves as the input to the PID controller, which produces the control signal based on the proportional, integral, and derivative actions. The controller output is subsequently scaled by a gain block before being applied to the plant, representing the micro-robotic system dynamics.

The SFOA operates as an external optimization layer within this closed-loop structure. During each iteration, candidate PID gain sets generated by the SFOA are applied to the controller. The resulting

system response is then simulated, and the corresponding error signal is computed. Based on this error signal, the ISTES objective function is evaluated and fed back to the SFOA as a fitness value. This evaluation–optimization cycle continues iteratively. The SFOA updates PID parameters by balancing exploration and exploitation, aiming to minimize the ISTES value. The optimization process continues until the predefined termination criterion is satisfied, typically the maximum number of iterations. Through this integrated framework, the controller tuning process is guided directly by closed-loop system behavior rather than relying on analytical approximations. The structure depicted in Figure 2 ensures that the optimized PID parameters are selected based on their actual impact on tracking performance, stability, and transient response characteristics of the micro-robotic position control system.

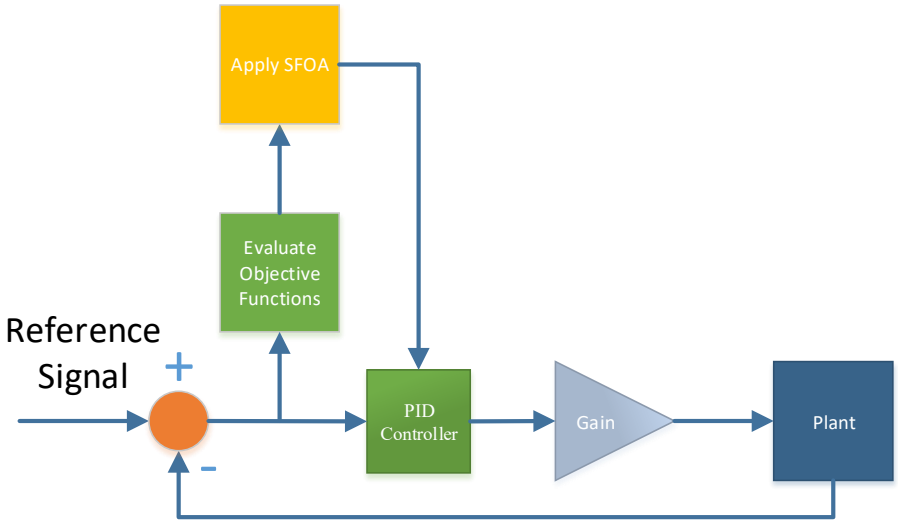


Figure 2. The implementation of the proposed control methodology based on SFOA

As illustrated in Figure 2, a constant gain block with a value of 0.003 is introduced between the PID controller output and the micro-robotic plant. This gain is incorporated to appropriately scale the PID controller's control signal before it is applied to the plant dynamics. The necessity of this gain arises from the physical characteristics and numerical scaling of the micro-robotic system model. Due to the extremely small mass and high sensitivity of the micro-particle dynamics, the plant exhibits a comparatively large response to small variations in the applied magnetic force. When the controller output is applied directly without scaling, excessively large control actions may result, leading to unrealistic actuation levels and numerical instability during simulation. By introducing a gain factor of 0.003, the magnitude of the control signal is adjusted to a physically meaningful range consistent with the micro-scale actuation forces achievable in practice. This scaling ensures that the closed-loop response remains stable, well-conditioned, and representative of realistic operating conditions, while preserving the relative influence of the optimized PID gains. Moreover, the adopted gain value has been selected in accordance with reported implementations of micro-robotic and micro-positioning control systems in the literature, where similar scaling factors are commonly employed to match controller outputs with plant actuation limits. Importantly, this gain is held fixed across all simulations, ensuring that the observed performance improvements are attributable solely to the optimized controller parameters rather than to additional actuation scaling.

5. RESULTS AND DISCUSSION

5.1. Adopted System Parameters

The physical and dynamic parameters adopted for the micro-robotic position control system are summarized in Table 1. These parameters were selected in accordance with values reported in the relevant literature on magnetically actuated micro-particle systems and low-Reynolds-number motion in viscous media. The adopted values are consistent with the modeling assumptions introduced in Section 2 and are commonly employed to represent realistic micro-robotic operating conditions [19].

Table 1. Adopted System Parameters for the Micro-Robotic Position Control System

Parameter	Symbol	Value	Unit
Particle radius	r_p	50	μm
Fluid density	ρ	998.2	kg·m^{-3}
Dynamic viscosity	η	1	mPa·s
Particle mass	m	7.33×10^{-10}	kg
Drag coefficient	C_d	0.94×10^{-6}	N·s·m^{-1}

The particle radius r_p corresponds to a micro-particle diameter of approximately $100\ \mu m$, which is in line with experimentally reported paramagnetic micro-particles used in magnetic manipulation studies. The fluid density ρ and dynamic viscosity η are chosen to reflect water-like liquid environments, as frequently assumed in micro-scale control and biomedical applications. These selections ensure that the flow regime remains laminar and that the Stokes drag approximation remains valid. The effective particle mass m and viscous drag coefficient C_d are also adopted from reported studies and directly influence the dynamic response of the system. These parameters are embedded in the continuous-time equation of motion and lead to the plant transfer function defined in Eq. (9). By substituting the parameter values listed in Table 1, the resulting plant model used in the simulations is obtained as follows.

$$G(s) = \frac{1}{7.33 \times 10^{-4} s^2 + 0.94\, s} \tag{20}$$

This transfer function accurately represents the inertial and viscous characteristics of magnetically actuated micro-particles in a fluid medium, as documented in the literature. By fixing these parameters throughout the study, the observed performance variations in the results section can be directly attributed to the proposed control and optimization strategy rather than to parameter tuning or modeling inconsistencies.

5.2. Simulation Setup

The simulation studies were conducted to evaluate the effectiveness and robustness of the proposed SFOA-based PID tuning strategy under standardized and reproducible conditions. To ensure a fair and meaningful comparison, the optimization process was carried out using the same experimental setup and parameter settings commonly adopted in related meta-heuristic control studies reported in the literature. The PID controller gains were treated as decision variables and constrained within predefined bounds to maintain physical feasibility and practical relevance. The search ranges for the controller parameters were defined as follows: the proportional gain was limited to $K_p \in [0{,}100]$, while the integral and derivative gains were constrained to $K_i \in [0{,}1]$ and $K_d \in [0{,}1]$, respectively [19]. These bounds were selected to provide sufficient flexibility for performance optimization while preventing excessively aggressive control actions.

For the SFOA implementation, the population size was fixed at 30 starfish, providing a balanced trade-off between search diversity and computational efficiency. The maximum number of iterations was set to 25, which was found to be adequate for convergence in similar optimization problems. To account for the stochastic nature of the algorithm and to ensure statistical reliability of the obtained results, each optimization experiment was independently repeated 25 times. During each run, the closed-loop micro-robotic position control system was simulated using the plant model defined in Section 2 and the system parameters listed in Table 1. The ISTES performance index defined in Eq. (19) was employed as the objective function, and its value was evaluated for each candidate PID parameter set generated by the SFOA. The optimization process proceeded until the termination criterion was satisfied, after which the best-performing controller parameters were recorded. By adopting consistent parameter bounds, population settings, and iteration limits across all runs, the simulation setup ensures that the reported results accurately reflect the optimization capability of the proposed approach rather than artifacts of parameter selection or experimental bias.

All simulation analyses were conducted for a step change in the reference position of 1000 μm. This displacement magnitude was selected to represent a realistic, practically relevant positioning task for micro-robotic manipulation systems, while remaining within the operating range of the adopted dynamic model and system parameters. By fixing the reference amplitude across all simulations and optimization runs, the closed-loop performance comparisons remain consistent and directly attributable to the control strategy rather than to variations in the commanded motion.

5.3. Statistical Results

To evaluate the robustness and consistency of the optimization process, a statistical analysis was conducted across multiple independent runs. Given the stochastic nature of meta-heuristic algorithms, such an analysis is essential to assess convergence reliability beyond single-run performance. The statistical evaluation was conducted using the ISTES objective function, which was identified as the primary performance index for the micro-robotic position control problem. A total of 25 independent optimization runs were executed under identical simulation conditions. For each run, the best objective function value obtained at the end of the optimization process was recorded. The resulting statistical indicators are summarized in Table 2, including the best, worst, mean, median, and standard deviation values. The extremely small variation between the best and worst outcomes, along with the low standard deviation, indicates a high degree of convergence, consistency, and robustness for the proposed optimization framework.

Table 2. Statistical performance of the proposed method

Metric	Value
Best	186,504,026.790784
Worst	186,504,285.639005
Mean	186,504,047.615164
Median	186,504,030.783154
Standard deviation	54.871955

To further contextualize the obtained results, a comparative numerical analysis was conducted using the best ISTES objective function values achieved by different optimization algorithms, as reported in the attached performance table. This comparison is intentionally limited to the objective function values in order to provide a clear and unbiased assessment of optimization effectiveness. For clarity, the optimization algorithms compared in Table 3 include the arithmetic optimization algorithm (AOA) [19], jellyfish search optimization (JS) [19], Harris hawks optimization (HHO) [19], and the hybrid arithmetic optimization algorithm with rat swarm optimization (HAOARSO) [19]. These methods were selected due to their widespread adoption and demonstrated effectiveness in control-oriented optimization problems reported in the literature.

As observed in Table 3, the proposed method achieves the lowest ISTES objective function value among all compared approaches. This result indicates superior suppression of time-weighted tracking errors and improved overall convergence behavior. When considered together with the statistical consistency demonstrated in Table 2, the findings confirm that the proposed optimization strategy not only enhances performance but also maintains strong robustness across repeated executions.

Table 3. Comparison of the best ISTES objective function values

Optimization algorithm	Best cost value
JS	186,946,887.68
HHO	187,684,604.20
AOA	186,687,807.46
HAOARSO	186,686,866.26
SFOA (Proposed)	186,504,026.79

5.4. Objective Function Evolution

The evolution of the objective function obtained using the proposed SFOA-based PID tuning approach is illustrated in Figures. 3 and 4, which provide complementary insights into the optimization behavior across multiple runs and iterations. Figure 3 depicts the best ISTES cost value achieved at the end of each independent run. As observed, the obtained cost values are tightly clustered around 1.865×10^8, with only minor deviations between runs. This narrow dispersion is consistent with the statistical indicators reported in Section 5.3 and confirms the strong repeatability and robustness of the proposed optimization framework. Although slight fluctuations are visible in a small number of runs, no systematic degradation or instability is observed, indicating that the stochastic components of the SFOA do not adversely affect convergence reliability.

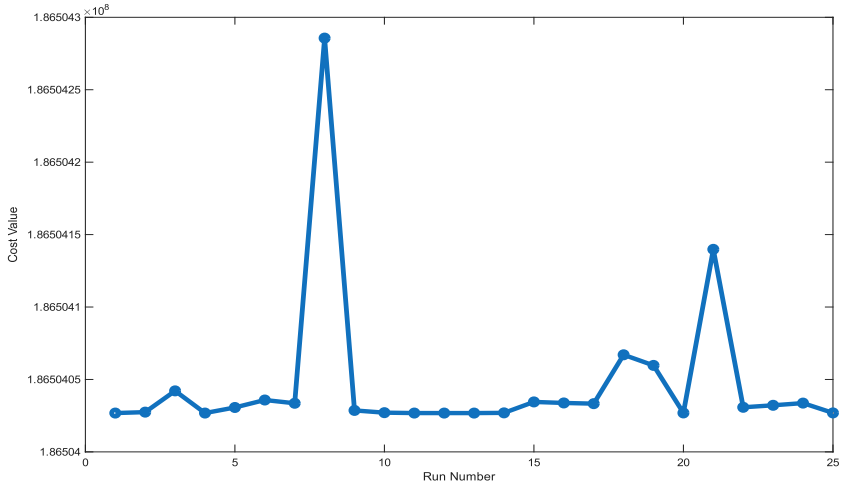


Figure 3. Cost values obtained after each run of the proposed method

Figure 4 presents the convergence curve corresponding to the best-performing run. A sharp reduction in the objective function is observed during the initial iterations, reflecting the strong global exploration capability of the SFOA in the early search phase. Following this rapid decrease, the convergence curve gradually flattens, indicating a transition from exploration to exploitation as the algorithm refines promising regions of the search space. After approximately the first few iterations, the cost value stabilizes and remains nearly constant until the termination criterion is reached. This behavior demonstrates that the algorithm is able to efficiently locate a high-quality solution and maintain convergence without oscillatory behavior or late-stage divergence.

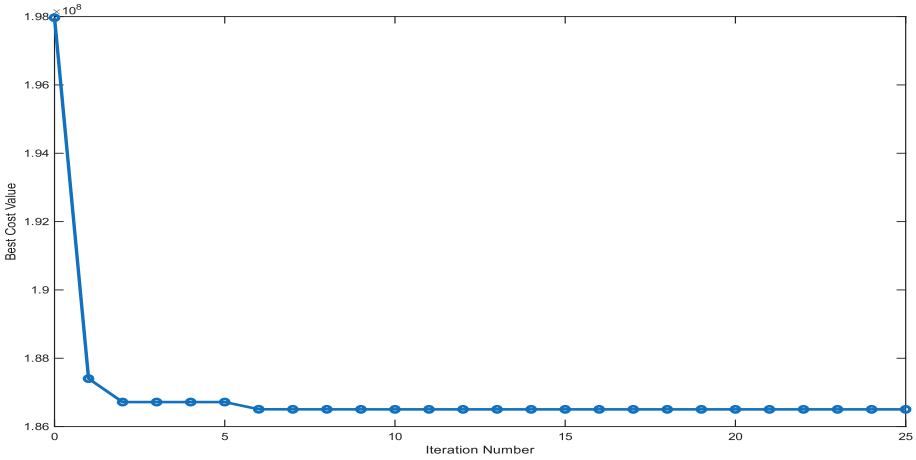


Figure 4. Convergence curve of the proposed method for the best run

5.5. Time Domain Response

The time-domain performance of the proposed SFOA-based PID controller was evaluated by applying a step change of 1000 μm to the reference position, and the resulting system response is illustrated in Figure 5. As observed, the micro-robotic position response exhibits a smooth and monotonic rise toward

the desired position, reaching the target displacement without oscillatory behavior. The trajectory demonstrates stable convergence and a well-damped transient response, indicating that the optimized PID gains effectively balance rapid tracking with stability requirements. Importantly, no overshoot is observed in the response, confirming the strong damping characteristics achieved through the proposed tuning strategy.

A quantitative comparison of time-domain performance indices is provided in Table 4, where the proposed method is evaluated against PID controllers tuned using JSO, HHO, AOA, and HAOARSO. As reported, the proposed SFOA-based PID controller achieves the shortest rise time of 6.8838 s and the lowest settling time of 12.0729 s among all compared approaches. More notably, the overshoot is completely eliminated, with a recorded value of 0.00%, whereas the competing algorithms exhibit nonzero overshoots ranging from 0.63% to 0.66%. These results clearly demonstrate that the proposed method enhances transient smoothness while preserving fast convergence. The absence of overshoot, along with competitive rise and settling times, highlights the effectiveness of ISTES-based optimization in shaping the closed-loop dynamics. By penalizing late-stage tracking errors more heavily, the controller is guided toward solutions that suppress residual oscillations and ensure gradual convergence to the reference position. Consequently, the proposed SFOA-based PID tuning approach delivers superior time-domain behavior, making it particularly suitable for precision-oriented micro-robotic positioning tasks where overshoot and oscillations must be strictly avoided.

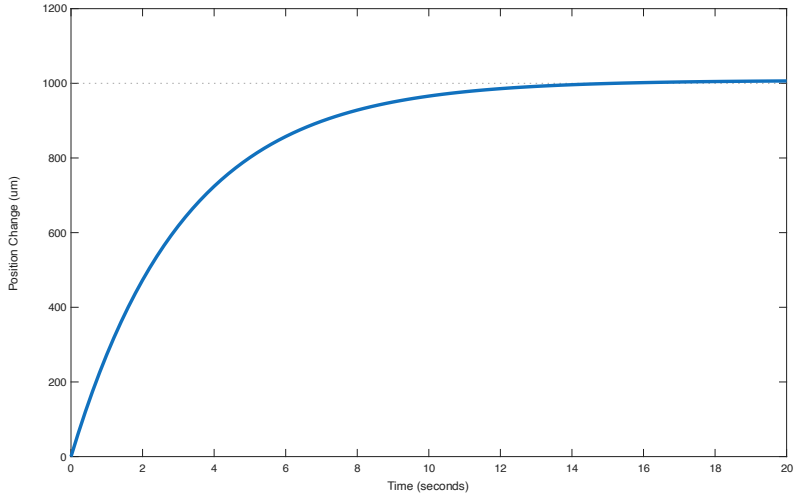


Figure 5. Step response of the proposed method for a position change of 1000 µm

Table 4. PID Characteristics of Algorithms

Algorithms	Rise time (s)	Settling time (s)	Overshoot (%)
JSO	6.8934	12.0796	0.66
HHO	6.8967	12.0910	0.63
AOA	6.8897	12.0746	0.64
HAOARSO	6.8896	12.0744	0.63
SFOA (Proposed)	6.8838	12.0729	0.00

6. CONCLUSION

In this study, an optimization-based control framework has been presented to enhance the transient and steady-state performance of a magnetically actuated micro-robotic position control system. The system dynamics were derived by considering the coupled effects of magnetic actuation and viscous drag acting on paramagnetic micro-particles suspended in a fluid medium, leading to a second-order dynamic model suitable for control design. To achieve accurate, overshoot-free position regulation, a classical PID controller was employed, with its parameters optimally tuned using the SFOA. The SFOA was integrated as an external optimization layer within the closed-loop control structure, allowing the controller gains

to be directly optimized based on the system's dynamic response rather than analytical approximations. The ISTES performance index was adopted as the objective function, ensuring strong penalization of late-stage tracking errors and promoting smooth transient behavior. The optimization process was conducted under standardized simulation conditions and independently repeated over multiple runs to assess robustness and convergence reliability. The results demonstrated that the proposed SFOA-based PID tuning strategy shows strong consistency, as reflected in the tightly clustered objective function values and the low standard deviation across independent runs. Convergence analyses confirmed that the algorithm rapidly locates high-quality solutions and maintains stable refinement throughout later iterations without oscillatory behavior. Time-domain evaluations further revealed that the proposed method produces a smooth, monotonic response to a 1000 μm step reference input, completely eliminating overshoot while achieving the shortest rise and settling times among the compared optimization-based PID approaches. Comparative analyses against controllers tuned using arithmetic optimization, jellyfish search optimization, Harris hawks optimization, and a hybrid arithmetic–rat swarm optimization algorithm clearly highlighted the superior transient smoothness and precision of the proposed approach. Overall, the findings indicate that the SFOA-based PID tuning framework provides an effective, reliable, and computationally efficient solution for high-precision micro-robotic positioning tasks. The ability to achieve overshoot-free operation with consistent transient performance makes the proposed method particularly suitable for applications where accuracy, stability, and smooth motion are critical. Future work may focus on experimental validation using real-time micro-robotic platforms, extending the approach to multi-axis positioning systems, and exploring hybrid or adaptive variants of the SFOA to further enhance performance under uncertainties and external disturbances.

Conflict of Interest Statement

There is no conflict of interest between the authors.

Statement of Research and Publication Ethics

The study is complied with research and publication ethics.

Artificial Intelligence (AI) Contribution Statement

This manuscript was entirely written, edited, analyzed, and prepared without the assistance of any artificial intelligence (AI) tools. All content, including text, data analysis, and figures, was solely generated by the authors.

Contributions of the Authors

Muhammet İsmail Güngör: Software, Simulation, Data curation, Visualization, Writing – original draft preparation. Davut İzci: Conceptualization, Methodology, Project administration, Supervision, Writing – review and editing. Serdar Ekinci: Methodology, Validation, Formal analysis, Writing – review and editing. Ehab Ghith: Investigation, Resources, Writing – review and editing.

REFERENCES

[1] T. Yoshikawa, K. Harada, A. Matsumoto, Hybrid position/force control of flexible-macro/rigid-micro manipulator systems, IEEE Transactions on Robotics and Automation 12 (1996) 633–640. https://doi.org/10.1109/70.508447.

[2] M.B. Khamesee, N. Kato, Y. Nomura, T. Nakamura, Design and control of a microrobotic system using magnetic levitation, IEEE/ASME Transactions on Mechatronics 7 (2002) 1–14. https://doi.org/10.1109/3516.990882.

[3] Yong Zhang, B.K. Chen, Xinyu Liu, Yu Sun, Autonomous Robotic Pick-and-Place of Microobjects, IEEE Transactions on Robotics 26 (2010) 200–207. https://doi.org/10.1109/TRO.2009.2034831.

[4] D. İzci, J. Hedley, Constructing an Electronic Circuitry for Label-free Hall Biosensors, Balkan Journal of Electrical and Computer Engineering 7 (2019) 366–372. https://doi.org/10.17694/bajece.633908.

[5] D. İzci, J. Hedley, Feasibility of Gold based Hall Devices for Biosensing Purposes, European Journal of Technic 10 (2020) 36–49. https://doi.org/10.36222/ejt.635719.

[6] D. Izci, C. Dale, N. Keegan, J. Hedley, The Construction of a Graphene Hall Effect Magnetometer, IEEE Sens. J. 18 (2018) 9534–9541. https://doi.org/10.1109/JSEN.2018.2872604.

[7] T. Hägglund, J.L. Guzmán, Give us PID controllers and we can control the world, IFAC-PapersOnLine 58 (2024) 103–108. https://doi.org/10.1016/j.ifacol.2024.08.018.

[8] E.S. Ghith, F. Abdel Aziz Tolba, Real-Time Implementation of Tuning PID Controller Based on Whale Optimization Algorithm for Micro-robotics System, in: 2022 14th International Conference on Computer and Automation Engineering (ICCAE), IEEE, 2022: pp. 103–109. https://doi.org/10.1109/ICCAE55086.2022.9762448.

[9] D. Izci, F. Artun, S. Ekinci, M. Bajaj, V. Blazek, I. Zaitsev, Enhanced Hiking Optimization Algorithm for Robust PID Control in Doubly-Fed Induction Generator Systems for Wind Energy Applications, IET Control Theory & Applications 19 (2025) e70071. https://doi.org/10.1049/cth2.70071.

[10] S. Ekinci, D. Izci, M. Yilmaz, Efficient Speed Control for DC Motors Using Novel Gazelle Simplex Optimizer, IEEE Access 11 (2023) 105830–105842. https://doi.org/10.1109/ACCESS.2023.3319596.

[11] W. Aribowo, E.S. Ghith, R. Rahmadian, M. Widyartono, A. Lukita Wardani, A. Prapanca, N.V. Laksmi B., Sand cat swarm optimization for controlling PID in DC motor, TELKOMNIKA (Telecommunication Computing Electronics and Control) 22 (2024) 462. https://doi.org/10.12928/telkomnika.v22i2.25630.

[12] D. Izci, E. Eker, S. Ekinci, M. Bajaj, V. Blazek, L. Prokop, Neighborhood centroid opposition-based flood algorithm for optimizing fractional-order PID control in nonlinear heat exchanger dynamics, Chaos Solitons Fractals 204 (2026) 117729. https://doi.org/10.1016/j.chaos.2025.117729.

[13] C. Turkeri, S. Ekinci, D. Izci, O. Kiselychnyk, FGO-Tuned 2-DOF PI controller for pressure regulation in centrifugal fans driven by induction motors using an experimentally validated model, ISA Trans. 169 (2026) 436–446. https://doi.org/10.1016/j.isatra.2025.12.012.

[14] E.S. Ghith, F.A.A. Tolba, Design and Optimization of PID Controller using Various Algorithms for Micro-Robotics System, Journal of Robotics and Control (JRC) 3 (2022) 244–256. https://doi.org/10.18196/jrc.v3i3.14827.

[15] B. Yağız, E. Eker, Y. Altun, Ş.N. Atar, D. Izci, S. Ekinci, M. Bajaj, M. Shabaz, Metaheuristic-Driven Optimization of a Neural Model Using Tuna Swarm Intelligence for Cognitive Classification of Wheat Species, International Journal of Computational Intelligence Systems 18 (2025) 292. https://doi.org/10.1007/s44196-025-01033-w.

[16] E.S. Ghith, F.A.A. Tolba, Tuning PID Controllers Based on Hybrid Arithmetic Optimization Algorithm and Artificial Gorilla Troop Optimization for Micro-Robotics Systems, IEEE Access 11 (2023) 27138–27154. https://doi.org/10.1109/ACCESS.2023.3258187.

[17] C. Zhong, G. Li, Z. Meng, H. Li, A.R. Yildiz, S. Mirjalili, Starfish optimization algorithm (SFOA): a bio-inspired metaheuristic algorithm for global optimization compared with 100 optimizers, Neural Comput. Appl. (2024). https://doi.org/10.1007/s00521-024-10694-1.

[18] D. Izci, S. Ekinci, M. Jabari, M. Bajaj, V. Blazek, L. Prokop, A.R. Yildiz, S. Mirjalili, A new intelligent control strategy for CSTH temperature regulation based on the starfish optimization algorithm, Sci. Rep. 15 (2025) 12327. https://doi.org/10.1038/s41598-025-96621-3.

[19] A. Baihan, E. Ghith, H. Garg, S. Mirjalili, D. Izci, M. Rashdan, M. Salman, K. Saleem, A Hybrid Meta-heuristic Algorithm for Optimum Micro-robotic Position Control with PID Controller, International Journal of Computational Intelligence Systems 18 (2025) 86. https://doi.org/10.1007/s44196-025-00799-3.

[20] E.S. Ghith, F.A.A. Tolba, LabVIEW Implementation of Tuning PID Controller Using Advanced Control Optimization Techniques for Micro-robotics System, International Journal of Mechanical Engineering and Robotics Research (2022) 653–661. https://doi.org/10.18178/ijmerr.11.9.653-661.

[21] D. Izci, F. Artun, S. Ekinci, R. Ghandour, M. Salman, E. Ghith, Design of PI–PDN Controlled DFIG System via a New Objective Function and Starfish Optimizer, in: 2025 9th International Symposium on Innovative Approaches in Smart Technologies (ISAS), IEEE, 2025: pp. 1–5. https://doi.org/10.1109/ISAS66241.2025.11101946.

[22] P. Cominos, N. Munro, PID controllers: recent tuning methods and design to specification, IEE Proceedings - Control Theory and Applications 149 (2002) 46–53. https://doi.org/10.1049/ip-cta:20020103.

[23] D. Izci, S. Ekinci, A. Demiroren, J. Hedley, HHO Algorithm based PID Controller Design for Aircraft Pitch Angle Control System, in: 2020 International Congress on Human-Computer Interaction, Optimization and Robotic Applications (HORA), IEEE, 2020: pp. 1–6. https://doi.org/10.1109/HORA49412.2020.9152897.